



## Journal of Advanced Research in Fluid Mechanics and Thermal Sciences

Journal homepage:  
[https://semarakilmu.com.my/journals/index.php/fluid\\_mechanics\\_thermal\\_sciences/index](https://semarakilmu.com.my/journals/index.php/fluid_mechanics_thermal_sciences/index)  
ISSN: 2289-7879



# Experimental Investigation on Thermal Performance of Solar Air Heater using Nano-PCM

Muntadher Mohammed Ali Saeed<sup>1,\*</sup>, Hassanain Ghani Hameed<sup>1</sup>, Hayder Azeez Neamah Diabil<sup>2</sup>

<sup>1</sup> Engineering Technical College, Najaf, Al-Furat Al-Awsat Technical University, 31001 Najaf, Iraq

<sup>2</sup> Mechanical Department, Engineering College, Kufa University, Najaf, Iraq

### ARTICLE INFO

#### Article history:

Received 12 December 2023

Received in revised form 9 April 2024

Accepted 20 April 2024

Available online 15 May 2024

#### Keywords:

Solar air heater; tube array-nano-PCM; flat plate solar collector; thermal performance of solar air heater

### ABSTRACT

Herein, the performance of a solar air heater (SAH) is experimentally investigated, utilising an array of tubes as the absorbent part. The study evaluates the impact of incorporating Al<sub>2</sub>O<sub>3</sub>-paraffin wax as a non-PCM storage medium in comparison to a traditional flat-plate solar air heater, specifically under Najaf-Iraq climate conditions. The SAH is positioned at an inclination of 32.1 degrees with respect to the horizon, allowing it to align optimally with the solar direction. The results reveal notable differences in thermal performance characteristics among the various models. The highest thermal efficiency values are observed for distinct configurations: the proposed model achieves about 55.2%, the wax-supported model reaches 55.9%, and the nano-PCM-reinforced model attains 57.7%, while the traditional model lags at 48.2%. Furthermore, an analysis of different air mass flow rates highlights a crucial finding. Specifically, an air mass flow rate of 0.01 kg/s results in a higher temperature exiting from the system compared to a flow rate of 0.02 kg/s. This is attributed to the extended interaction time between the passing air and the absorbing surface, facilitating enhanced heat exchange. Consequently, the system's thermal efficiency experiences an increase. The study underscores the superior thermal performance and efficiency of the tube array nano-PCM collector type under Najaf city-Iraq climate conditions.

## 1. Introduction

Solar radiation can be utilised by converting it into a form of useful energy such as chemical, potential, or thermal energy. One of the widest applications of solar energy is solar collectors, which are designed to convert solar radiation into useful heat capable of heating homes and buildings. May used with these collectors' different storage materials. In general, the type of thermal storage material is chosen based on the amount of energy required for storage. In solar energy equipment, the amount of thermal storage is controlled by several factors, such as the amount of available solar energy, the type of load, and the type and specifications of the storage materials used. From previous

\* Corresponding author.

E-mail address: [muntadher.a17@yahoo.com](mailto:muntadher.a17@yahoo.com)

<https://doi.org/10.37934/arfmts.117.1.8397>

factors, the appropriate design of the system is obtained, such as storage medium size at the lowest cost [1-3].

Many solar energy applications have been studied, such as solar air heaters, water heaters, water desalination, and air-drying systems [4-8]. Solar air heaters have many unique features; they do not suffer from freezing, leakage, or the accumulation of salt problems. In addition, it is easy to install and low-cost [9,10]. Kabeel *et al.*, [11] presented a review study that reviewed many different studies in terms of geometric design, shape of the absorbent part, and use of two-phase thermal storage materials. The results obtained showed that the use of two-phase materials with different properties has the ability to increase the thermal efficiency of the system. Lin *et al.*, [12] conducted a practical study that included the use of pure paraffin wax in the process of storing thermal energy to heat closed buildings, which effectively affected the process of storing and rationalizing solar energy consumption. Air heating systems can be obtained using a lot of designs based on solar energy storage using paraffin wax and its mixtures [13-15].

Many authors have used PCM in a variety of applications of solar energy storage and release [16-18]. Mahmud *et al.*, [19] theoretically investigated the improvement of a solar air heater's thermal efficiency. Their study includes an absorbent body consisting of an array of tubes filled with a mixture of paraffin wax and 5% aluminium nanoparticles as a phase change material. Their results showed that the gain in air temperature due to the process of thermal energy discharge decreases with increasing air mass flow rate, and the freezing time for this compound takes a long-time interval for the lower mass flow rates. In order to perform a theoretical analysis of a solar air heater, Kumar *et al.*, [4] used a phase change material (PCM) made of a homogeneous mixture of paraffin wax and aluminium powder. With a high value of 29.86%, Muthukumaran and Senthil [20] reported an improvement in thermal efficiency using the spiral tubes of a solar air heater loaded with a glycerol and paraffin mixture. Jawad *et al.*'s [21] work carried out their research in Baghdad, Iraq, which has a particular climate. The results showed that the mixture's thermal conductivity increased by about 18.3%, allowing the solar air heater to operate for an additional three hours after dusk. El-Fakharany *et al.*, [22] presented a practical discussion study that included the use of a solar air heater with a flat absorption plate reinforced with a bottom layer of paraffin, and a group of vacuum air tubes were integrated into the solar absorption plate. The results showed that there was an increase in the percentage of accumulated useful energy that ranged from 13 to 16% when using paraffin wax. Rawat and Sherwani [23] presented a simulation study focusing on finding out the best ratio of the thickness of the PCM layer to its length for a single- and double-pass solar air heater, where it was shown that increasing the ratio of the thickness of the PCM layer to its length worked to delay the thermal discharge of the system, which leads to raising the energy and system efficiency. The highest discharge efficiency reached 63.34% with a thickness-to-length ratio of about 0.058% for the double-pass heater. Balakrishnan *et al.*, [24] presented a practical study that included the design and testing of a solar air heater equipped with an absorption plate embedded with rectangular fins and a layer of paraffin wax. Experimental results show that incorporating PCM at the bottom of the absorber plate effectively reduces energy loss and raises outlet temperatures, resulting in a 0.36-year energy recovery period and reducing carbon emissions by approximately 0.34 tons per year.

From the studies reviewed above, we note that there are few studies presented within the climate in southern Iraq regarding solar air heaters of various designs and knowledge of the best ones, so work is underway to present this practical study.

In this work, the performance of a solar air heater with tube array was studied under the influence of climatic conditions to the Iraqi city of Najaf, and the effect of adding a Nano-paraffin wax block on the efficiency of the system during sunrise or at sunset. The experimental results of the system (with and without PCM and with Nano-PCM) were compared with a conventional flat-black plate collector

(FPC) model of similar dimensions and under the same climatic conditions. The effect of changing the speed of the air inlet on the productivity of the model was also studied, to know how successful this application is within the conditions of this city.

## 2. Mathematical Background

A storage medium such as salt water, stone, or oil that changes its temperature in response to an active external temperature can be used to store thermal energy. Conversely, latent thermal energy, like that obtained from the melting of paraffin wax, is stored in phase-changing materials. The amount of stored sensible thermal energy units is greater than the amount of latent solar thermal energy units. It is also possible to store thermal energy by making use of chemical reactions. The most important arithmetic operations that govern the process of converting sensible thermal energy into latent energy are as follows [25,26]

$$Q = m \cdot L \tag{1}$$

where, m = mass of PCM [kg] and L = specific latent heat of PCM [J/kg].

The thermal efficiency of the model can be calculated as follows

$$\eta = \frac{\dot{m}c_p (\Delta T)}{A_c G} \tag{2}$$

where,

$\dot{m}$  = Air mass flow rate (kg/s),

$C_p$  = Air specific heat (J/kg. K)

While  $\Delta T = T_o - T_i$  and  $T_o, T_i$  = outlet and inlet air temperature of SAH ( $^{\circ}\text{C}$ ), respectively.

Also, G = Radiation intensity ( $\text{W} / \text{m}^2$ ), and  $A_c$  = Area of SAH ( $\text{m}^2$ ).

## 3. Preparation of $\text{Al}_2\text{O}_3$ -Wax Mixture

A rigorous technique is employed to provide optimal outcomes when preparing the  $\text{Al}_2\text{O}_3$ -wax mixture. Table 1 shows the properties of paraffin wax and  $\text{Al}_2\text{O}_3$  nanoparticles.

**Table 1**

Properties of paraffin wax and  $\text{Al}_2\text{O}_3$  nanoparticles

Property	PW	$\text{Al}_2\text{O}_3$
Density ( $\text{kg}/\text{m}^3$ )	$\rho_s = 880$ $\rho_l = 770$	3600
Specific heat ( $C_p$ ) ( $\text{J}/\text{kgK}$ )	2000	765
Thermal conductivity ( $\text{W}/\text{mK}$ )	$k = 0.2$	36
Viscosity ( $\mu$ ) ( $\text{Ns}/\text{m}^2$ )	$0.001 \exp(-4.25+1790/T)$	-----
Latent heat (L) ( $\text{J}/\text{kg}$ )	160	-----
Melting Temperature ( $^{\circ}\text{C}$ )	56	-----

Firstly, the wax undergoes a regulated heating procedure, gradually increasing its temperature to 60°C until it completely melts. Afterwards, a precise amount of 3% volume of Al<sub>2</sub>O<sub>3</sub> is carefully added to the melted wax, guaranteeing complete and even distribution. The amalgam is subsequently poured into a 1000-ml pyrex vial that is hermetically sealed, thus establishing a controlled environment for the following procedures. The hermetically sealed vial is placed within an ultrasonic bath, namely the Elmasonic P180H, manufactured by Elma in Germany (Figure 1). To ensure optimal ultrasonic performance, it is essential to maintain a water level that is 5 cm higher than the mixture. The ultrasonic bath operates constantly for a duration of eight hours, ensuring that the physical conditions are maintained at a temperature of 65°C and a frequency of 37 Hz. The strict time and precise conditions are essential to ensuring the creation of a uniform mixture of Al<sub>2</sub>O<sub>3</sub> and wax, resulting in the necessary qualities for the intended use. This technique guarantees accuracy and consistency in the preparation of the wax blend infused with nano-Al<sub>2</sub>O<sub>3</sub>, which can be used for future applications.



**Fig. 1.** Pictorial view of the sonicator, Elmasonic - P180H - Elma, Germany

#### 4. Experimental Setup

The experimental model was designed and built (with specifications shown in Table 2), as shown in Figure 2, in the Energy Research Unit at Najaf Engineering Technical College.

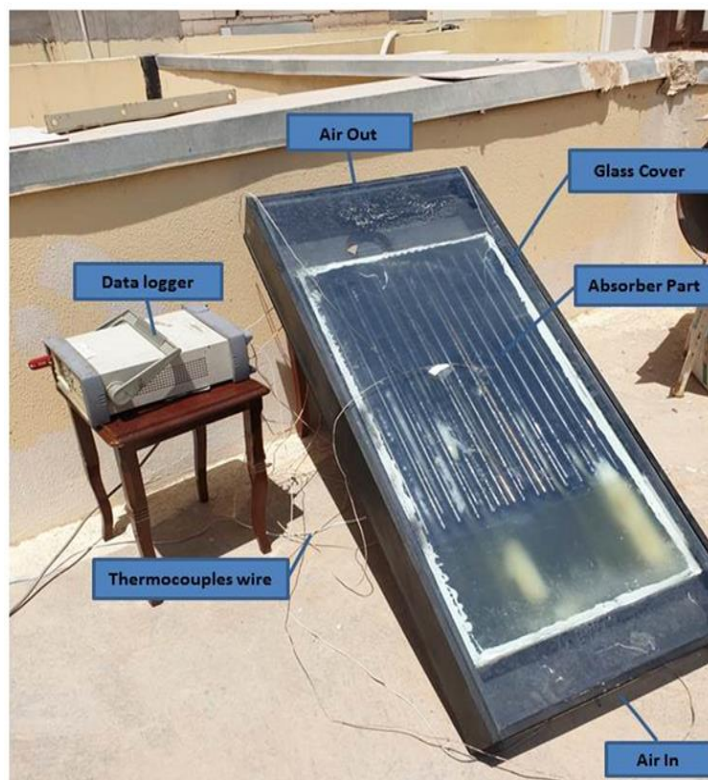


Fig. 2. Tube array heating unit

Table 2

Experimental unit specifications

Component	Specification
Wooden bed	MDF wood box with dimensions of 54.2cm as width and 119cm as length
Glass Cover	Traditional glass with thickness of 0.4cm, width of 54.2cm, length of 119cm and transmissivity of 0.88
Rig stand	Wooden stand with a tilt angle of 32.1 degrees
External insulation	glass wool insulator with thermal conductivity of 0.033W/m.K and thickness of 5cm
K-type thermocouple	Use at three locations (entry, exit and inside the wax layer)
Rechargeable battery	Small size rechargeable battery with specifications of 4.5 amps and 12 volts
Pipes	Copper tube, with number of 13, diameter of 1.905cm, length of 90cm and thickness of 1mm
Fan	Electrical Fan model with 129 CFM, 120 mm frame, 12V and 1.3 AMP.
Paraffin wax	13.5kg, with Melting temperature of 56 °C, thermal conductivity of 0.2 W/m.K and solid to liquid density of 880 to 770 kg/m <sup>3</sup> .
Al <sub>2</sub> O <sub>3</sub>	Density of 3600kg/m <sup>3</sup> , Specific heat (Cp) of 765 J/kg.K, and Thermal conductivity of 36W/m.K.

In this rig (model A), solar radiation passes through the transparent glass covering to the absorbent part (pipes) (A1), PCM layer (paraffin wax) (A2), or Nano-PCM (Al<sub>2</sub>O<sub>3</sub>-paraffin wax) layer (A3), surrounding the absorbent part, which consists of 13 hollow copper tubes that allow air to pass through them. The absorbent part is painted a matte black color to increase the absorption of short waves of solar radiation. At the upper end of the wooden bed installed for all parts of the system, a fan is installed to draw the hot air stream passing through the absorption surface. At sunrise, the solar radiation is transmitted through the glass cover to the paraffin or Al<sub>2</sub>O<sub>3</sub>-paraffin wax layer, which absorbs it and leads to its almost complete melting, and the rest of the heat is transmitted to

the absorbent part by conduction, which leads to heating the air passing through it. At sunset, there is little or no incoming radiation; heat is transferred from the nano-wax layer to the absorbent part (pipes), which causes the air to continue heating for as long as possible. At the same dimensions and climatic conditions, another conventional model that uses a flat plate as an absorbent part (model B), as shown in Figure 3, was built in. A fan with 12 volts is placed at the outlet port for the two models to get rid of turbulent flow problems and create different flow pressure levels during its operation, which leads to the passage of air through the pipes (the absorbent part). The results obtained from model A are compared with those of model B. Table 3 shows the physical characteristics of the solar heating system.

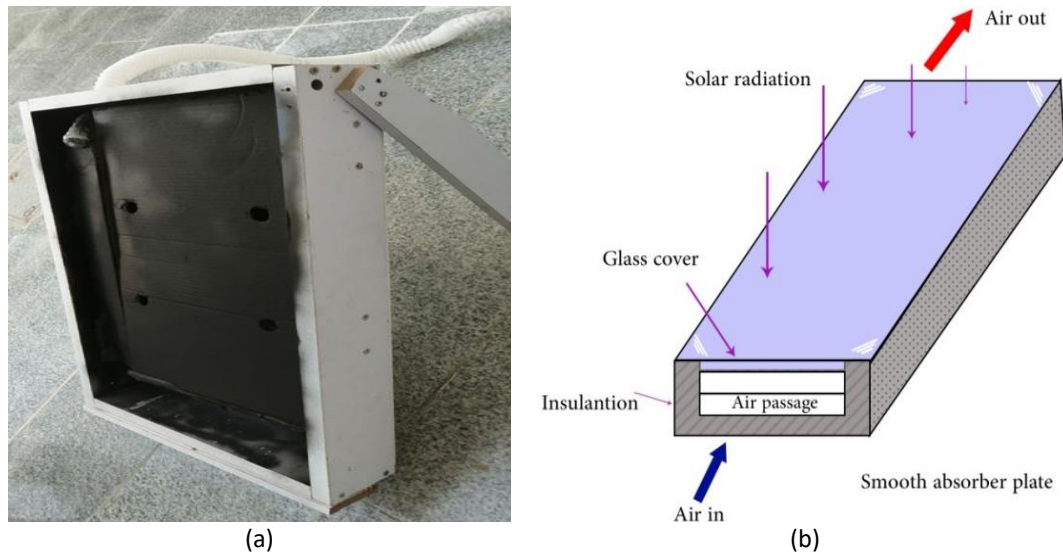


**Fig. 3.** Flat plate heating unit, (a) experimental device, and (b) schematic illustration of the heating unit

During the experimental work, several devices' measurements have been used. Temperatures are measured at various points within the experimental rig using K-Type thermocouple with measurement accuracy of  $(0.2\% \pm 1 \text{ } ^\circ\text{C})$ . All thermocouples connect to a 32 channel digital display thermometer (AT-4532x), which is illustrated in Figure 4(a). An electronic solar radiation meter, as shown in Figure 4(b), with model of (TM-207) and accuracy of  $(\pm 5\% \pm 10 \text{ W/m}^2)$  is used in this experiment. Temperature data for various parts and the amount of air mass flow passing through the device were recorded in the practical experiment after calibrating all measuring devices and knowing the appropriate procedures, as the percentage of uncertainty in this research was less than 5%. Table 4 shows the estimated values of uncertainty.



**Table 3**  
 Physical characteristics of the solar heating system

No.	Design specifications for parameters and materials	
Collector Parts		
1	Tilt angle	32.1°
2	Transparent cover area	Traditional glass with thickness of 0.4cm, width of 54.2cm, length of 119cm and transmissivity of 0.88
3	Absorption plate	A cast iron metal plate with a thickness of 2 mm and an area of 0.447m <sup>2</sup>
4	Container box	MDF wood box with dimensions of 54.2cm as width and 119cm as length
5	Insulation	glass wool insulator with thermal conductivity of 0.033W/m.K and thickness of 5cm
Storage Part		
1	Pipe	Copper tube, with number of 13, diameter of 1.905cm, length of 90cm and thickness of 1mm
2	Paraffin wax weight	13.5 kg
3	Alumina nanoparticles concentration	3 Vol.%

**Table 4**  
 Uncertainty of Experimental Data

Parameters	Errors %
Mass flow rate	0.44
Temp.	0.2
Solar radiation intensity meter	3.7



**Fig. 4.** Applents Digital Data Logger Thermometer (AT-4532x) 32 Channel type (a), and (b) Solar radiation measurement device (Pyranometer)

## 5. Results and Discussion

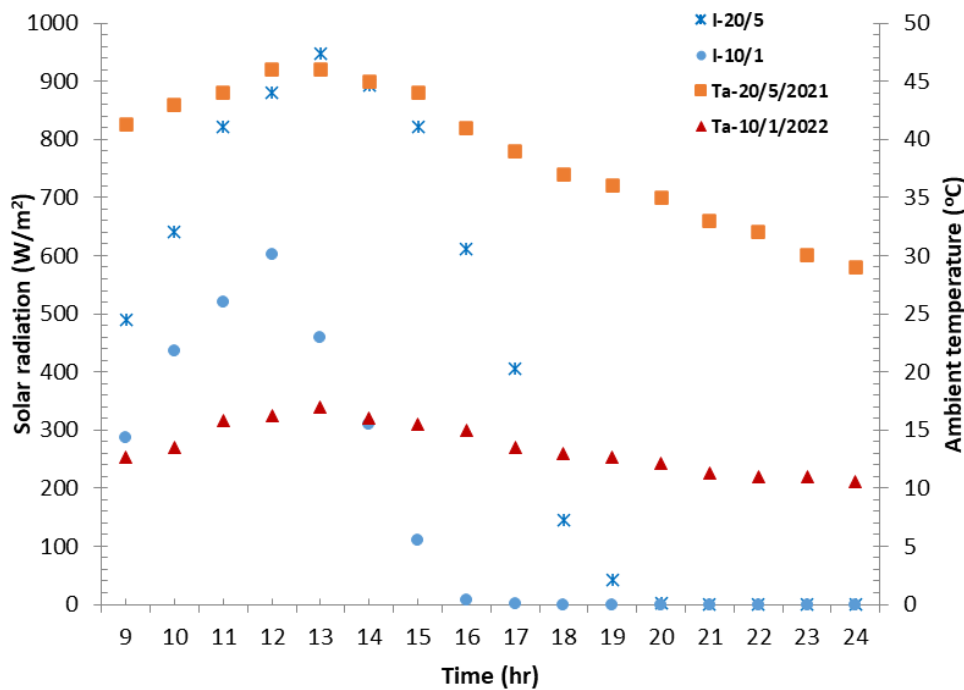
In this work, all experimental tests were conducted in the city of Najaf (31.2° latitude and 43.9° longitudinal) on May 20, 2021, and January 10, 2022, with an interval time of 8 a.m. until 12 a.m. for an air flow rate of 0.01 and 0.02 kg/s. The thermal efficiency values for both current models were listed in Table 5 on May 20, 2021.

Figure 5 shows the behaviour of ambient temperature and solar radiation with the time of the experiments on 5/2021 and 10/1/2022. It is clear from the figure that the solar radiation increases with time until it reaches its maximum value (948 W/m<sup>2</sup>) at noon (1 pm) and then decreases until it reaches its minimum value at the beginning of sunset.

The data depicted in Figure 6 and Figure 7 demonstrates the temporal fluctuations of temperatures in various sections of a solar collector system on May 20, 2021, with variable air flow rates of 0.01 and 0.02 kg/s. The temperature profiles consistently show an ascending trend until reaching a high at 14:00 pm, followed by a subsequent decrease, mirroring the pattern of solar intensity throughout the day. A notable result is the negative correlation between temperature values and the rate of air flow. This suggests that the duration of contact between the air and the walls of the tube in the collector influences heat exchange.

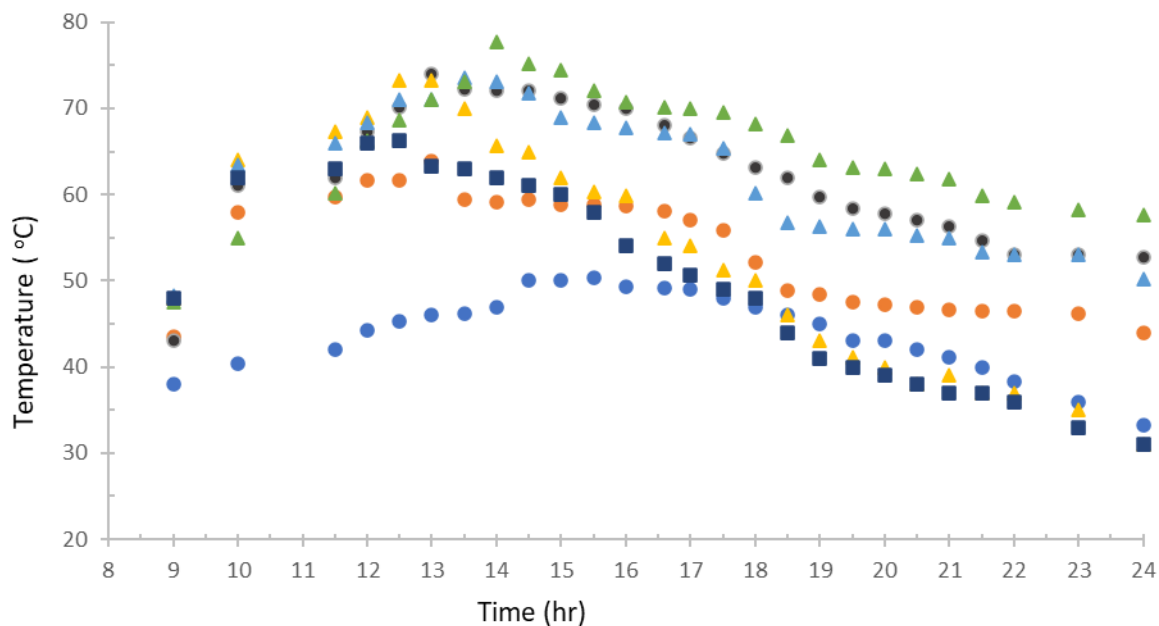
**Table 5**  
 Thermal efficiency values of models under consideration

Time (hr)	Thermal Efficiency (%) for 0.01kg/s				Thermal Efficiency (%) for 0.02kg/s			
	Model-A			Model-B (Flat plate)	Model-A			Model-B (Flat plate)
	A1-Without PCM	A2-With PCM	A3-With Nano-PCM		A1-Without PCM	A2-With PCM	A3-With Nano-PCM	
9	32	31.1	31.1	31.3	30	30	30	30.1
10	46.1	44.3	42.8	45.2	44.0	41.1	41.0	42.6
11	53.2	51	46.5	49.7	51.9	49.3	45.1	44.5
12	55.2	53.6	49.7	50.1	52.7	50.6	47.6	46.8
13	54.2	55.9	53.3	48.2	50.5	54.1	51.3	44.2
14	53.0	55.3	57.7	45.2	49.6	53.3	54.3	43.1
15	50	54.6	57	43.1	47.9	52.1	54.1	40.2
16	43.7	53.9	57	38.1	40.6	51.2	54	33.3
17	36.6	53.4	55.8	33.9	33.8	51.4	53.1	30.7
18	21.9	44.7	55	14.2	19.3	41.7	45.4	11.6
19	14.6	42.3	53.1	7.3	12.6	37.1	41.2	4.9
20	7.4	41.1	46	3.1	5.0	34.2	40.3	0
21	4.8	36.9	41.2	0	2.1	31.5	38.5	0
22	3.1	33.2	39.1	0	0	29.7	34.3	0
23	0	33.1	36.2	0	0	26.5	32.4	0
24	0	29.9	35	0	0	22.1	30.1	0

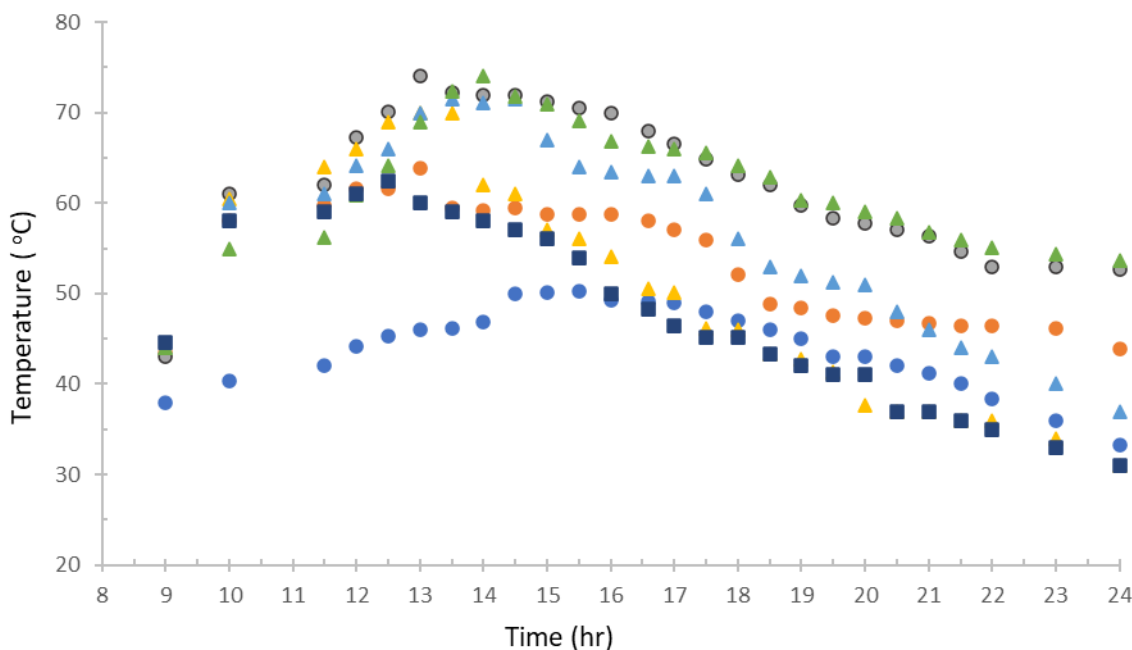


**Fig. 5.** Relationship between temperature and solar radiation with time





● T-glass ● T-PCM ● T-NPCM ▲ Tout - without PCM ▲ Tout - with PCM ▲ Tout - with NPCM ■ Tout - FPC  
**Fig. 6.** Behavior of temperatures along the two models for air mass flow rate of 0.01 kg/s on 20/5/2021



● T-glass ● T-PCM ● T-NPCM ▲ Tout - without PCM ▲ Tout - with PCM ▲ Tout - with NPCM ■ Tout - FPC  
**Fig. 7.** Behavior of temperatures along the two models for air mass flow rate of 0.02 kg/s on 20/5/2021

The utilisation of Phase Change Material (PCM) or Nano Phase Change Material (NPCM) is found to be a crucial factor in increasing temperatures, especially during the afternoon and extending the operational duration of the solar collector after sunset, as indicated by the graphical representations. When comparing the results, the highest temperatures achieved with the Fluidized Particle Bed Collector (Flat plate collector) are 66.3 and 62.5 °C, but with NPCM, they increase to 77.7 and 74.1 °C for air flow rates of 0.01 and 0.02 kg/s respectively. PCM and NPCM play a crucial role in improving the performance and efficiency of the solar collector system.

In addition, the results depicted in Figure 8 and Figure 9 emphasise the changes in temperature over time under different experimental settings on 10/1/2022, with a specific focus on air flow rates of 0.01 and 0.02 kg/s. The temperature differences found demonstrate consistent trends among the outlets that do not have Phase Change Material (PCM), outlets with PCM, outlets with Nano Phase Change Material (NPCM), and outlets made of Foamed Polymer Concrete (Flat plate collector). The similar behaviour observed in Figure 6 and Figure 7, despite the same air flow rates, demonstrates the reliability of the models. However, the different temperature values in Figure 8 and Figure 9 emphasise the impact of the winter season on the experimental results. The results highlight the crucial influence of solar radiation and air variables on the thermal performance of the system.

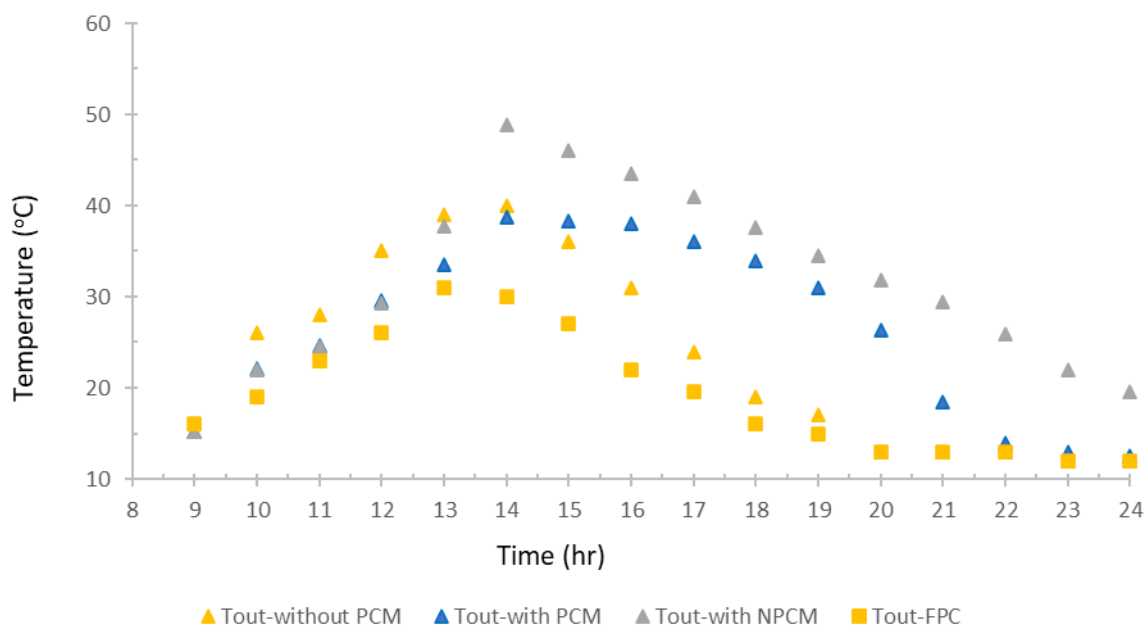


**Fig. 8.** Behavior of temperatures along the two models for air mass flow rate of 0.01 kg/s on 10/1/2022

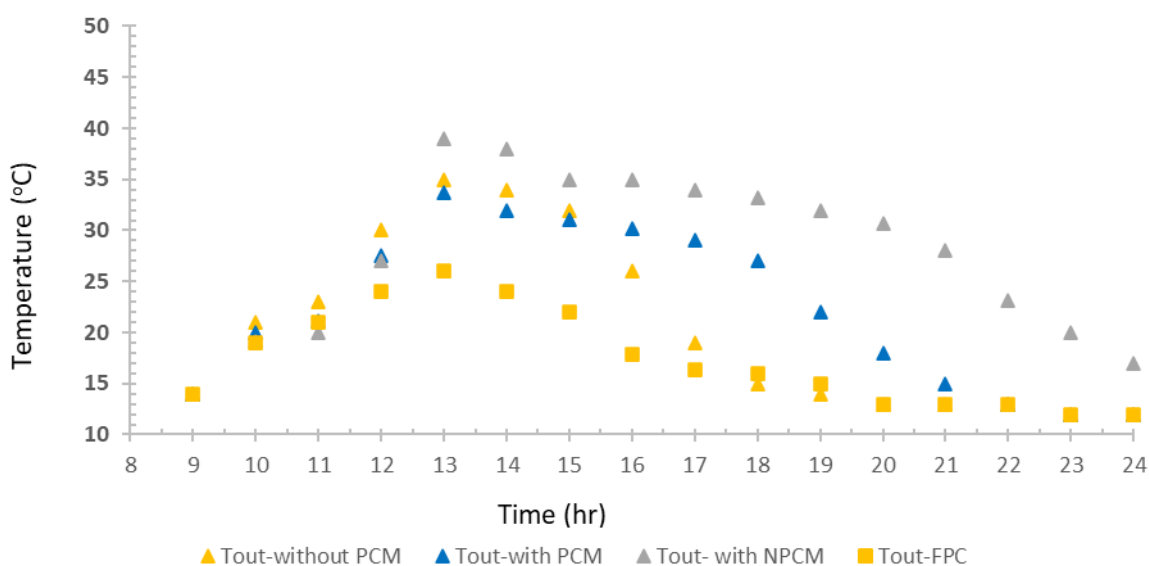
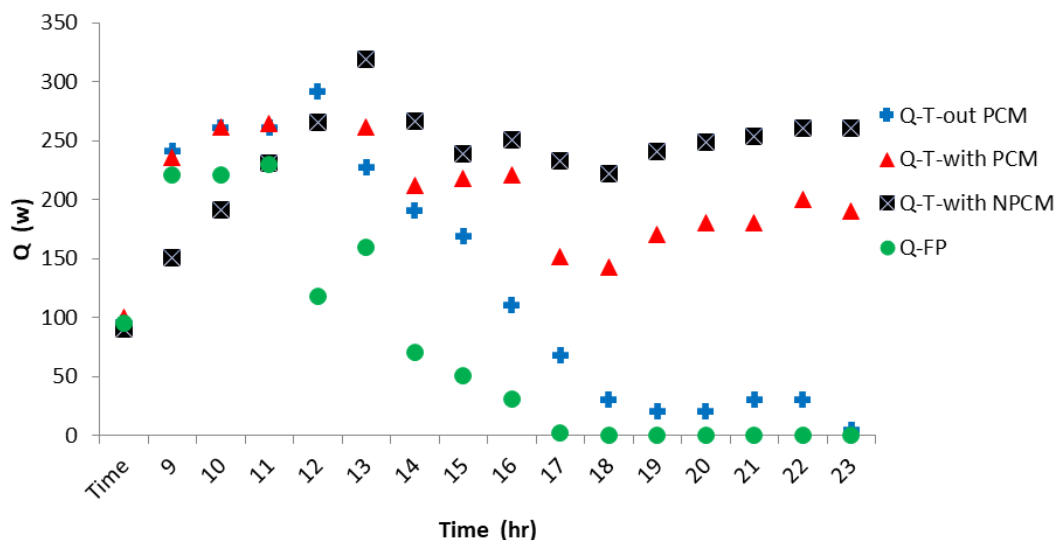


**Fig. 9.** Behavior of temperatures along the two models for air mass flow rate of 0.02 kg/s on 10/1/2022

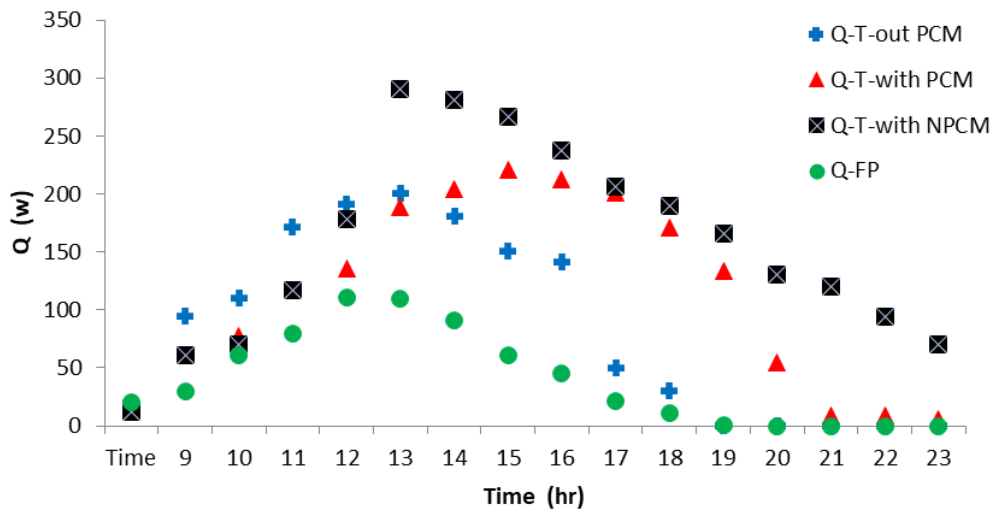
The highest documented output temperatures for FPC are 31 and 26 °C, whereas NPCM reaches temperatures of 48.8 and 39 °C for air flow rates of 0.01 and 0.02 kg/s, respectively. The significant influence of material selections on the thermal behaviour of the system is highlighted by this difference, offering vital insights for the future investigation and improvement of solar thermal applications.

Figure 6 and Figure 7 show the observed change in inlet and outlet temperatures with different air flow rates for all models used. For the black plate model, it is noted that the method of distributing the outgoing temperature is similar when using different masses of incoming air. The maximum temperature is observed at 1 pm as shown in Figure 5. The reason for this is that the amount of solar radiation reaches its maximum value at noon. A similar scheme can be observed for the exit temperature distribution for the tubular model with or without paraffin wax. As shown in Figure 6, we notice that a decrease in the amount of passing air leads to a higher exit temperature at all times of the experiment because there is more time for the exchange of heat transfer from the tubes to the air. This can be shown for each model. By noting all models, A and B, Where the highest output air temperature was at Model A3, it is 78.3, 74.2°C, with an air mass flow rate of 0.1 kg/s and  $m = 0.2$  kg/s, respectively. For the same air mass flow rates, the lowest temperatures of the air leaving the model were recorded at 56.8 and 53.3 °C, respectively. Also, for the model A2 and at the same air mass flow rates, the highest temperatures of the air leaving the model were recorded at 73 and 71°C, respectively. The NPCM-enhanced tube heater gives more heat output than the other three models.

From practical experience, the traditional solar heater (model B) was examined, and the results were compared with the proposed tubular heaters (models A1, A2, and A3). In Model A1, the improvement of the surface heat exchange leads to a significant increase in the output temperature. Thus, there is an increase in the thermal efficiency of the model. This is clearly shown in Figure 10, Figure 11, and Figure 12, which show changes in the amount of heat transfer (watts) and the time-varying thermal efficiency values for models B, A1, A2, and A3, respectively.



**Fig. 10.** Behavior of rate of heat transfer along the two models for air mass flow rate of 0.01 kg/s on 20/5/2021



**Fig. 11.** Behavior of rate of heat transfer along the two models for air mass flow rate of 0.01 kg/s on 10/1/2022

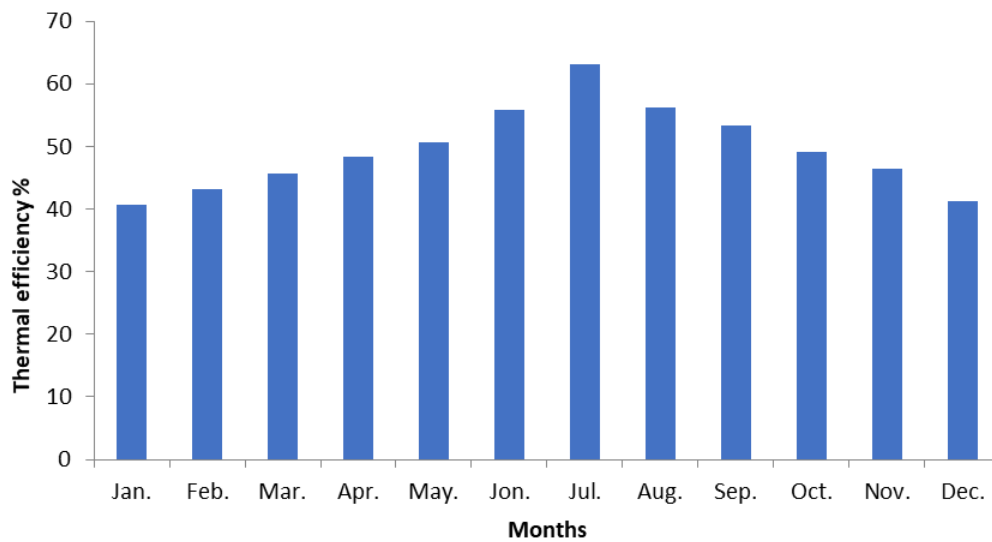


**Fig. 12.** Behavior of thermal efficiency of the model A3 over the year for an air mass flow rate of 0.01 kg/s

The results of this work closely correspond to the findings reported by Sharma *et al.*, [27], illustrating the ability of phase change materials (PCMs) to improve the thermal efficiency of solar air heaters. This is corroborated by Jawad *et al.*, 's [21] results, who used nano-PCMs in a synergistic way to successfully increase a solar air heater's efficiency. They provide important insights for the development of sustainable and effective heating systems in the future. From Figure 12, it notices that the highest amount of enhancement in thermal efficiency for Model A3 is 63.14% in the seventh month, when the length of the solar day is the greatest possible and the value of the solar radiation is the highest compared to the other months of the year. On the other hand, the amount of enhancement in thermal efficiency was the least, and it was approximately 40.8% in the first month of the year, where solar radiation is less intense and the length of the solar day is shorter compared to the other months of the year, which reduces the amount and time of heat exchange between the mass of air passing through the matrix of heat-absorbing pipes. This graph was drawn based on the practical experience of Model 3 on specific days of each month within the real atmosphere of the Iraqi city of Najaf and during the period extending from April 13, 2021, to May 17, 2022.

## 6. Conclusions

The current study focused on the creation and construction of a solar air heater (SAH) that uses an array of black tubes as the component responsible for absorbing heat. The work sought to improve heat retention and enhance thermal efficiency by incorporating paraffin wax and  $\text{Al}_2\text{O}_3$  as a means of storing thermal energy, and the performance was compared with a conventional air heater. The experiments were conducted under real meteorological conditions in Najaf, Iraq, resulting in the subsequent important discoveries

- i. The study showed that it is possible to use solar radiation to melt a phase-change material, which can be used as a medium for storing heat. This technique enables subsequent air heating during periods of reduced solar radiation intensity.
- ii. There was clear and observable evidence of heat transfer from the absorption plate to the air that was flowing through. This was especially noticeable when analysing the temperature difference between the air entering and exiting the system.
- iii. The utilisation of a phase-change material guarantees the long-term retention of heat from solar radiation, allowing for an extended duration of air heating during sunset.
- iv. The use of the mixture consisting of the phase change material with nanoparticles led to an increase in the temperature of the outlet air and a prolongation of the device's production time for hot air due to the higher thermal conductivity of the mixture compared to the use of the phase change material alone.
- v. Thermal efficiency values were calculated for various models, including the proposed model, wax-supported model, nano-PCM-reinforced model, and traditional model. The thermal efficiencies achieved by these models were approximately 55.2%, 55.9%, 57.7%, and 48.2%, respectively.
- vi. Remarkably, a decrease in the air mass flow rate from 0.02 kg/s to 0.01 kg/s led to an increase in the system's exit temperatures. The prolonged duration of contact between the flowing air and the surface that absorbs it resulted in an augmented transfer of heat and a heightened level of thermal efficiency.
- vii. The addition of  $\text{Al}_2\text{O}_3$  nanoparticles enhanced the conductivity of the phase-change material, leading to faster thermal absorption, dissolution of the phase-change material, heat storage, and heat exchange processes.

This research highlights the effectiveness of a solar air heater model that uses an array of black copper tubes as a heat absorption plate, while the thermal storage of the model is enhanced using paraffin wax and a mixture of paraffin wax and aluminium oxide nanoparticles individually. The output was compared to that of a conventional air heater. The experiments were conducted under specific climatic conditions in the city of Najaf, Iraq. The results provide useful information for selecting the most efficient solar air heater type for practical use in similar environmental conditions.

## References

- [1] He, Zhaoyu, Abdul Samad Farooq, Weimin Guo, and Peng Zhang. "Optimization of the solar space heating system with thermal energy storage using data-driven approach." *Renewable Energy* 190 (2022): 764-776. <https://doi.org/10.1016/j.renene.2022.03.088>
- [2] Saxena, Abhishek, Erdem Cuce, Desh Bandhu Singh, Muneesh Sethi, Pinar Mert Cuce, Atul A. Sagade, and Avnish Kumar. "Experimental studies of latent heat storage based solar air heater for space heating: A comparative analysis." *Journal of Building Engineering* 69 (2023): 106282. <https://doi.org/10.1016/j.jobee.2023.106282>
- [3] Salunkhe, Pramod B. "Investigations on latent heat storage materials for solar water and space heating applications." *Journal of Energy Storage* 12 (2017): 243-260. <https://doi.org/10.1016/j.est.2017.05.008>

- [4] Kumar, Atul, Prabhakar Bhandari, and K. S. Rawat. "Numerical simulation of solar air heater using paraffin wax-aluminum compound as phase changing material." *Aptisi Transactions on Technopreneurship (ATT)* 3, no. 2 (2021): 164-170. <https://doi.org/10.34306/att.v3i2.199>
- [5] El Khadraoui, Aymen, Salwa Bouadila, Sami Kooli, Amenallah Guizani, and Abdelhamid Farhat. "Solar air heater with phase change material: An energy analysis and a comparative study." *Applied Thermal Engineering* 107 (2016): 1057-1064. <https://doi.org/10.1016/j.applthermaleng.2016.07.004>
- [6] Mahmood, Abdulrahman Shakir. "Experimental study on double-pass solar air heater with and without using phase change material." *Journal of Engineering* 25, no. 2 (2019): 1-17. <https://doi.org/10.31026/j.eng.2019.02.01>
- [7] Lubis, Hamzah. "Renewable energy of rice husk for reducing fossil energy in Indonesia." *Journal of Advanced Research in Applied Sciences and Engineering Technology* 11, no. 1 (2018): 17-22.
- [8] Khattak, Muhammad Adil, Mohammad Azfar Haziq Ayoub, Muhammad Ariff Fadhllillah Abdul Manaf, Mohd Faidhi Mahru, Mohd Ridwan Mohd Juhari, Mira Idora Mustaffa, and Suhail Kazi. "Global energy security and European Union: A review." *Journal of Advanced Research in Applied Sciences and Engineering Technology* 11, no. 1 (2018): 64-81.
- [9] Hu, Jianjun, Kaitong Liu, Long Ma, and Xishan Sun. "Parameter optimization of solar air collectors with holes on baffle and analysis of flow and heat transfer characteristics." *Solar Energy* 174 (2018): 878-887. <https://doi.org/10.1016/j.solener.2018.09.075>
- [10] Hu, Jianjun, and Guangqiu Zhang. "Performance improvement of solar air collector based on airflow reorganization: A review." *Applied Thermal Engineering* 155 (2019): 592-611. <https://doi.org/10.1016/j.applthermaleng.2019.04.021>
- [11] Kabeel, Abd Elnaby, Mofreh H. Hamed, Z. M. Omara, and A. W. Kandeal. "Solar air heaters: Design configurations, improvement methods and applications-A detailed review." *Renewable and Sustainable Energy Reviews* 70 (2017): 1189-1206. <https://doi.org/10.1016/j.rser.2016.12.021>
- [12] Lin, Wenye, Zhenjun Ma, Haoshan Ren, Jingjing Liu, and Kehua Li. "Solar thermal energy storage using paraffins as phase change materials for air conditioning in the built environment." *Paraffin: an Overview* (2020): 1-15. <https://doi.org/10.5772/intechopen.86025>
- [13] Shareef, Abbas Sahi, Farhan Lafta Rashid, and Hasan Fathi Alwan. "Water solar distiller productivity enhancement using solar collector and phase change material (PCM)." In *IOP Conference Series: Materials Science and Engineering*, vol. 671, no. 1, p. 012150. IOP Publishing, 2020. <https://doi.org/10.1088/1757-899X/671/1/012150>
- [14] Shareef, Abbas Sahi, Farhan Lafta Rashid, Aseel Hadi, and Ahmed Hashim. "Water-polyethylene glycol/(SiC-WC) and (CeO<sub>2</sub>-WC) nanofluids for saving solar energy." *International Journal of Scientific & Technology Research* 8, no. 11 (2019): 1041-1043.
- [15] Rashid, Farhan Lafta, Aseel Hadi, Ammar Ali Abid, and Ahmed Hashim. "Solar energy storage and release application of water-phase change material-(SnO<sub>2</sub>-TaC) and (SnO<sub>2</sub>-SiC) nanoparticles system." *International Journal of Advances in Applied Sciences* 8, no. 2 (2019): 154-156. <https://doi.org/10.11591/ijaas.v8.i2.pp154-156>
- [16] Rashid, Farhan L., Shahid M. Talib, Aseel Hadi, and Ahmed Hashim. "Novel of thermal energy storage and release: water/(SnO<sub>2</sub>-TaC) and water/(SnO<sub>2</sub>-SiC) nanofluids for environmental applications." In *IOP Conference Series: Materials Science and Engineering*, vol. 454, no. 1, p. 012113. IOP Publishing, 2018. <https://doi.org/10.1088/1757-899X/454/1/012113>
- [17] Hadi, Aseel, Farhan Lafta Rashid, Hasan Qahtan Hussein, and Ahmed Hashim. "Novel of water with (CeO<sub>2</sub>-WC) and (SiC-WC) nanoparticles systems for energy storage and release applications." In *IOP Conference Series: Materials Science and Engineering*, vol. 518, no. 3, p. 032059. IOP Publishing, 2019. <https://doi.org/10.1088/1757-899X/518/3/032059>
- [18] Al-Garah, Naheda Humood, Farhan Lafta Rashid, Aseel Hadi, and Ahmed Hashim. "Synthesis and characterization of novel (organic-inorganic) nanofluids for antibacterial, antifungal and heat transfer applications." *Journal of Bionanoscience* 12, no. 3 (2018): 336-340. <https://doi.org/10.1166/jbns.2018.1538>
- [19] Mahmud, Alkilani, K. Sopian, M. A. Alghoul, and Mat Sohif. "Using a paraffin wax-aluminum compound as a thermal storage material in a solar air heater." *ARPJ Journal of Engineering and Applied Sciences* 4, no. 10 (2009): 74-77.
- [20] Muthukumar, Jayaraman, and Ramalingam Senthil. "Experimental performance of a solar air heater using straight and spiral absorber tubes with thermal energy storage." *Journal of Energy Storage* 45 (2022): 103796. <https://doi.org/10.1016/j.est.2021.103796>
- [21] Jawad, Qusay A., Aedah MJ Mahdy, Ahmed H. Khuder, and Miqdam T. Chaichan. "Improve the performance of a solar air heater by adding aluminum chip, paraffin wax, and nano-SiC." *Case Studies in Thermal Engineering* 19 (2020): 100622. <https://doi.org/10.1016/j.csite.2020.100622>
- [22] El-Fakharany, Magda K., Aly-Eldeen A. Abo-Samra, A. M. Abdelmaqsoud, and S. A. Marzouk. "Enhanced performance assessment of an integrated evacuated tube and flat plate collector solar air heater with thermal

- storage material." *Applied Thermal Engineering* (2024): 122653. <https://doi.org/10.1016/j.applthermaleng.2024.122653>
- [23] Rawat, Piyush, and Ahmad Faizan Sherwani. "Optimization of single and double pass solar air heater-phase change material (SAH-PCM) system based on thickness to length ratio." *International Journal of Heat and Mass Transfer* 224 (2024): 125356. <https://doi.org/10.1016/j.ijheatmasstransfer.2024.125356>
- [24] Balakrishnan, Paramasivam, Senthil Kumar Vishnu, Jayaraman Muthukumaran, and Ramalingam Senthil. "Experimental thermal performance of a solar air heater with rectangular fins and phase change material." *Journal of Energy Storage* 84 (2024): 110781. <https://doi.org/10.1016/j.est.2024.110781>
- [25] Mohamad, Ahmad Tajuddin, Nor Azwadi Che Sidik, and M'hamed Beriache. "Thermo physical enhancement of advanced nano-composite phase change material." *Journal of Advanced Research in Applied Mechanics* 54, no. 1 (2019): 1-8.
- [26] Kalidasan, B., A. K. Pandey, Saidur Rahman, Kamal Sharma, and V. V. Tyagi. "Experimental investigation of graphene nanoplatelets enhanced low temperature ternary eutectic salt hydrate phase change material." *Energies* 16, no. 4 (2023): 1574. <https://doi.org/10.3390/en16041574>
- [27] Sharma, Ashutosh, Ranchan Chauhan, Mehmet Ali Kallioğlu, Veerakumar Chinnasamy, and Tej Singh. "A review of phase change materials (PCMs) for thermal storage in solar air heating systems." *Materials Today: Proceedings* 44 (2021): 4357-4363. <https://doi.org/10.1016/j.matpr.2020.10.560>